Stretch-induced quenching in flame-vortex interactions

By J.-M. Samaniego

1. Motivation and objectives

The flame-vortex interaction problem is a natural configuration in which several issues relevant to turbulent combustion can be addressed: effect of strain-rate and curvature, effect of the Lewis number, effect of heat losses, effect of complex chemistry, and flame-generated turbulence (Jarosinski *et al.* 1988, Rutland and Ferziger 1991, Poinsot *et al.* 1991, Roberts and Driscoll 1991, Roberts *et al.* 1993, Wu and Driscoll 1992, Lee *et al.* 1993, Lee and Santavicca 1993). In such an approach, the interaction of an isolated vortex with a laminar premixed flame is viewed as a unit process of a turbulent premixed flame in which the reaction zone keeps a laminar-like structure locally; this is precisely the case of the wrinkled flame or flamelet regime in turbulent combustion (Williams 1985, Borghi 1988).

Poinsot *et al.* 1991 have carried out numerical simulations of a two-dimensional flow field where a vortex pair is convected through a laminar premixed flame. The authors identified three regimes of interaction depending on the ratios u_θ/S_l and d/δ_l (where u_θ and d are the velocity perturbation and size of the vortex pair, and S_l and δ_l are the flame speed and flame thickness): 1) for small values of u_θ/S_l and d/δ_l, the flame front is nearly unaffected; 2) for an intermediate range of these parameters, the flame front is wrinkled and pockets of unburnt mixture surrounded by burnt gases are formed; 3) for higher values, the flame front can be locally quenched in the presence of heat losses. These results were confirmed by experimental observations (Roberts and Driscoll 1991, Roberts *et al.* 1993).

The present work complements previous studies and involves the study of the interaction of a vortex pair and a laminar premixed flame in a planar two-dimensional geometry, together with numerical simulations. This geometry is quite unique since most studies have considered axisymmetric vortex rings. Such a geometry offers several advantages over previous studies:

- line-of-sight measurement techniques such as schlieren flow visualization, CH emission imaging, and infrared emission imaging can be used in order to obtain quantitative data: schlieren flow visualization can be used to determine the flame surface area; imaging of the light emission from electronically excited CH radicals in the reaction zone can be used to infer the reaction rate field (John and Summerfield 1957, Diederichsen and Gould 1965, Hurle *et al.* 1968, Poinsot *et al.* 1987, Yip and Samaniego 1992, Samaniego *et al.* 1993); near-infrared emission from water vapor in the $700-1200\,nm$ range can be used to obtain the temperature field in the burnt gases. In addition, laser-based diagnostics such as particle image velocimetry to measure the velocity field or Rayleigh scattering as an alternative way of measuring the temperature field can be applied.

- ensemble-averaging of several realizations can be performed in order to improve the signal-to-noise ratio.
- quantitative comparisons with a two-dimensional code described in Poinsot *et al.* 1991 can be undertaken. This would allow to separately study the effects of non-unity Lewis numbers, heat losses, and complex chemistry. In particular, the validity and applicability of reduced chemical schemes for direct numerical simulation of turbulent premixed flames can be tested.
- in parallel to the single events where an isolated vortex pair interacts with a premixed flame, multiple vortex-flames interactions can be studied as an example of single-scale turbulence-flame interactions.

This paper presents initial experimental results of flame-vortex interactions. It is shown that, under certain circumstances, the flame undergoes a quenching-reignition process where quenching is associated to an excessive stretching of the flame front.

2. Accomplishments

2.1 Experimental facility

An experimental facility with a two-dimensional flow has been developed. The test section comprises a vertical duct with a square cross-section of $63.5 \times 63.5\,mm$, equipped with quartz windows for optical access (see Fig. 1). A mixture of propane or methane and air is fed into the test section through a contoured converging nozzle. Combustion is stabilized on an electrically-heated Nichrome wire of $0.5\,mm$ diameter, resulting in a V-shaped flame. A vortex pair is generated by acoustic excitation through a $3\,mm$ wide contoured slot located in the left wall. At time $t = 0$, a single pulse is sent to the speaker. The pulse is generated by filtering and amplifying a TTL pulse. The resulting signal is a ramp with a rise time of $1\,ms$. The slot has a rectangular shape and spans the entire lateral wall. In the present study, the aspect ratio of the slot was approximately 21 : 1. Conceptually, the resulting vortex pair is two-dimensional, spans the entire test section, and is parallel to the Nichrome wire. As a consequence, the flow field during a flame-vortex interaction is expected to be two-dimensional.

Several parameters control the interaction of the vortex with the flame, including the type of fuel, the equivalence ratio (ϕ), the flow velocity of the fuel-air stream (V_0), the flame thickness (δ_l) and flame speed (S_l), the size of the vortex core (d_c), and the maximum rotational velocity of the vortex (u_θ). Using methane or propane allows possible Lewis number (Le) effects to be investigated.

In the absence of velocity measurements, it is difficult to give a definite value for the maximum velocity perturbation u_θ induced by the vortex pair. However, based on smoke visualizations of the vortex pair in the absence of flame, a schematic diagram of the vortex pair has been developed (Fig. 2) (Samaniego 1993). In this case, the following relationship holds: $u_\theta = 4V_d$, where V_d is the self-induced velocity of the vortex pair.

Qualitative flow visualization showing both the position of the vortex pair and of the flame during the interaction has been performed with a schlieren arrangement.

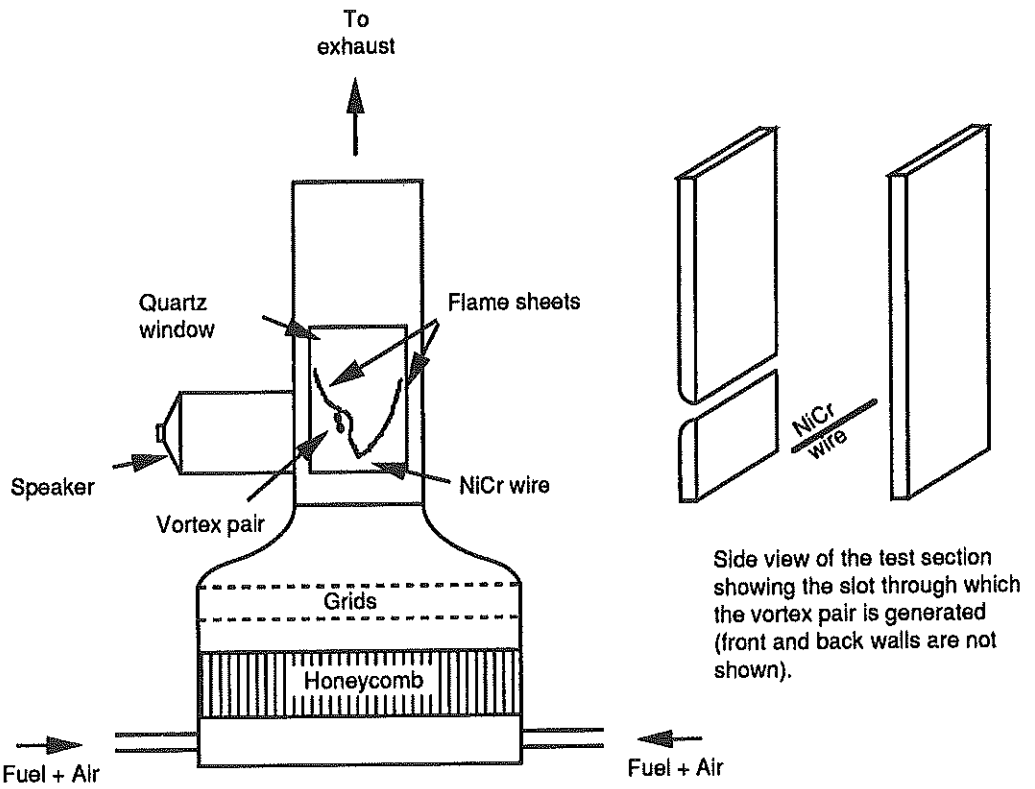

FIGURE 1. Schematic view of the test section.

The light source was a flashlamp delivering $0.1\,ms$ duration pulses. The schlieren image was recorded by a TM540 PULNIX video camera and VCR. The images were later digitized on a PC AT equipped with a DT-2851 digitizing board. A timing circuit allowed delaying the light pulse from the vortex generation so that images could be taken at different instants during the interaction.

Global emission measurements were done using a Hamamatsu 1P28A photomultiplier tube equipped with an interference filter isolating light emission from CH radicals from the $^2\Delta \rightarrow {}^2\Sigma$ transition at $431.5\,nm$. A second PC AT equipped with a DT-2828 acquisition board was used to digitize the photomultiplier signal (typically, 1000 samples at a rate of $10,000\,samples/s$). Acquisition was synchronized with the vortex generation event.

2.2 Results and discussion

2.2.1 Schlieren flow visualization

Figure 3 shows a sequence of schlieren images of a flame-vortex interaction along with the overall reaction rate. This latter quantity was inferred from the CH

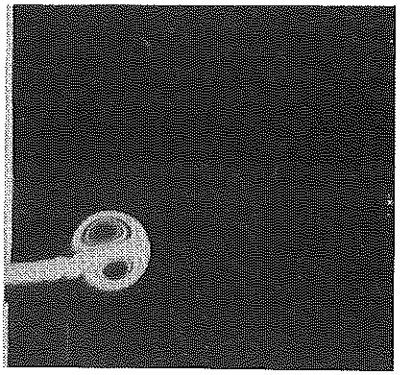

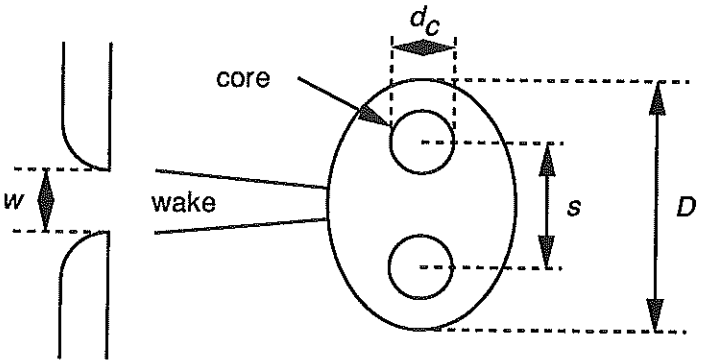

FIGURE 2. Vortex pair topology. a) light sheet illumination of a smoke pattern (from Samaniego 1993) - b) schematic diagram of the vortex pair.

emission from the entire flame. Fifty realizations were averaged and the standard deviation computed in order to check the repeatability of the interaction. In this case, the operating conditions are: fuel=C_3H_8, $\phi = 0.55$, $V_0 = 0.35\,m/s$, $\delta_l = 1\,mm$, $S_l = 0.12\,m/s$, $d_c = 3\,mm$, $u_\theta = 24\,m/s$, $Le = 1.8$, resulting in $u_\theta/S_l = 200$, $d/\delta_l = 3$.

The first image shows the position of the unperturbed V-shaped flame. The flame is slightly curved towards the burnt gases due to confinement. The second image is taken $4.8\,ms$ after acoustic excitation. A starting vortex pair is rolling-up. The flame already senses the presence of the vortical structure and starts straightening out. This can be attributed to mass-conservation and to a Biot-Savart effect induced

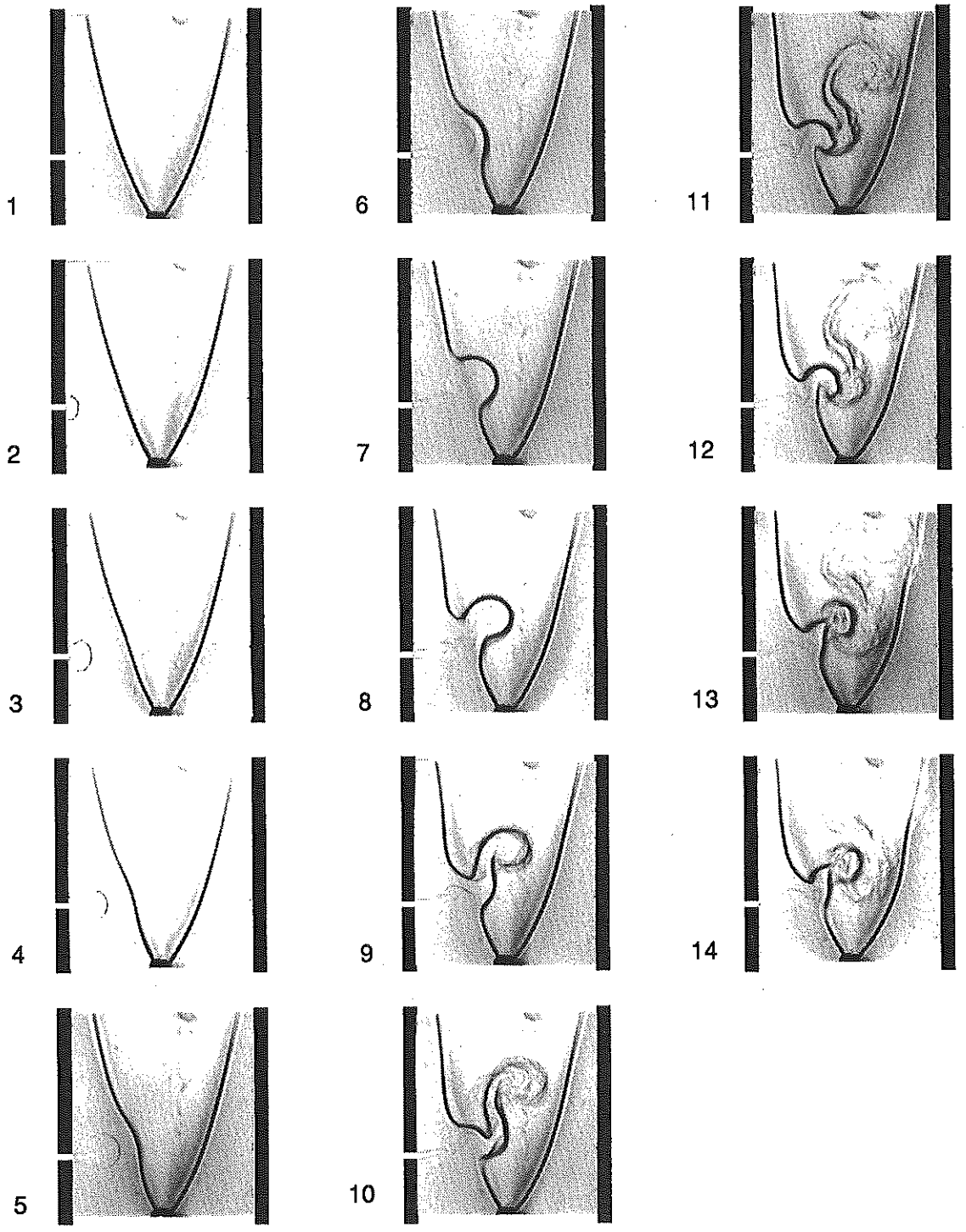

FIGURE 3a. Sequence of schlieren images. See caption on next page for more details.

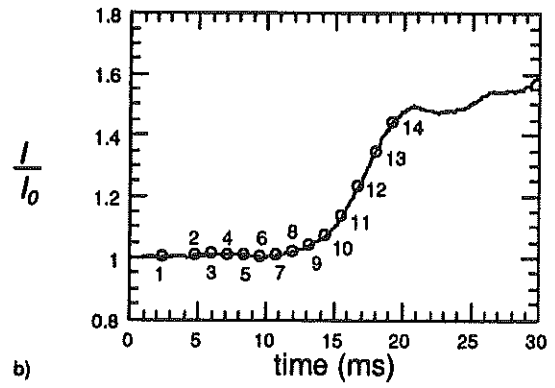

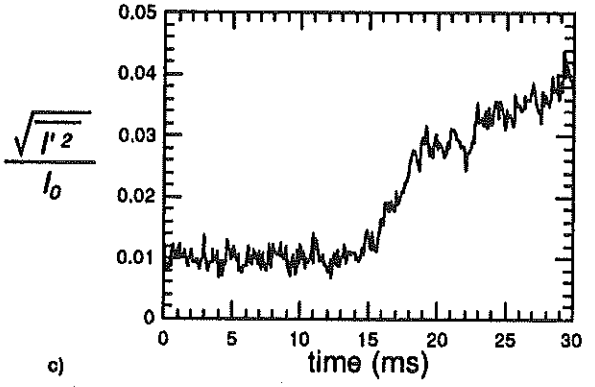

FIGURE 3. Flame-vortex interaction: fuel= C_3H_8, $\phi = 0.55$, $V_0 = 0.35\,m/s$, $\delta_l = 1\,mm$, $S_l = 0.12\,m/s$, $d_c = 3\,mm$, $u_\theta = 24\,m/s$, $Le = 1.8$ ($u_\theta/S_l = 200$, $d_c/\delta_l = 3$). a) Sequence of schlieren photographs showing the evolution of the reacting flow field (see previous page) - b) evolution of the corresponding I/I_0, where I is the mean global CH emission averaged over 50 realizations, and I_0 is the initial value of I. The numbered circles correspond to the schlieren photographs - c) evolution of $\sqrt{\overline{I'^2}}/I_0$, where $\sqrt{\overline{I'^2}}$ is the standard deviation of I, the global CH emission signal computed from 50 realizations, and I_0 is the initial value of I.

by the vortex pair. The next 12 images are taken $1.2\,ms$ apart and show the evolution of the flame-vortex interaction.

From both the schlieren pictures and the standard deviation of the photomultiplier signal, two phases of the flame-vortex interaction can be identified: 1) an initial phase lasting until approximately $t = 13.2\,ms$, where the flow field is two-dimensional and repeatable, and during which the flame surface area increases while the reaction rate remains constant; 2) a second phase in which the flow field starts becoming three-dimensional, is less repeatable, and during which the reaction rate increases significantly.

During the first phase, the vortex pair propagates toward the flame front and reaches it at $t = 10.8\,ms$. The flame front becomes more distorted as the vortex follows its path. The arc length of the flame contour increases steadily, while the reaction rate remains nearly constant. The vortex pair is followed by a wake featuring a Kelvin-Helmholtz instability.

The second phase starts at $t = 13.2\,ms$, when the schlieren image becomes blurred around the vortex pair. In the vortex wake is an elongated flame front which also becomes blurred at $t = 15.6\,ms$. This phase is characterized by a 40% increase of the overall reaction rate. The blurring of the schlieren pattern is due to combustion within the vortex pair.

The existence of two phases compares well with previous results obtained by Jarosinski *et al.* 1988, for the interaction of a vortex bubble with an upward propagating laminar flame. The authors associated each phase of the interaction with a physical mechanism and a time scale: first, a mixing time, τ_m, during which entrainment of burnt material into the vortex core takes place, then a combustion time, τ_c, after ignition of the vortex core. They found that τ_c is weakly dependent on the mixture composition of the vortex and that $\tau_c \simeq \tau_m$. They concluded that the interaction is essentially controlled by fluid mechanical processes. Jarosinski *et al.* speculated that, during the first phase, the flame front is quenched by excessive stretching ahead of the vortex bubble. This assumption is checked and proved to be correct in the following section. However, the way combustion is initiated in the second phase and the structure of the reaction zone during this ignition process, whether it is flamelet-like or distributed over a volume, are still unknown.

2.2.2 Flame quenching and Lewis number effect

In order to address the issue of whether or not the flame front is locally quenched, the relationship between the flame surface area, Σ, and the overall reaction rate, W, is investigated. For this purpose, Σ was deduced from the arc length of the flame contour measured on the schlieren images. Only the images taken in the first phase, where the flow field is two-dimensional, have been considered.

It appears that W lags Σ by about 5 milliseconds (Fig. 4). Furthermore, while Σ increases by 40 %, W remains within 1% of its initial value. Since the reaction zone is flamelet-like during the first part of the interaction, as demonstrated by the schlieren pictures, W can be defined as follows:

$$W = \int_{\Sigma} \omega ds$$

where ω is the local burning rate per unit surface. If we assume that ω is constant then

$$W = \omega \Sigma$$

and W is proportional to Σ which is in contradiction with the observation. Consequently, ω must decrease locally in order to balance the increase of Σ. This can be

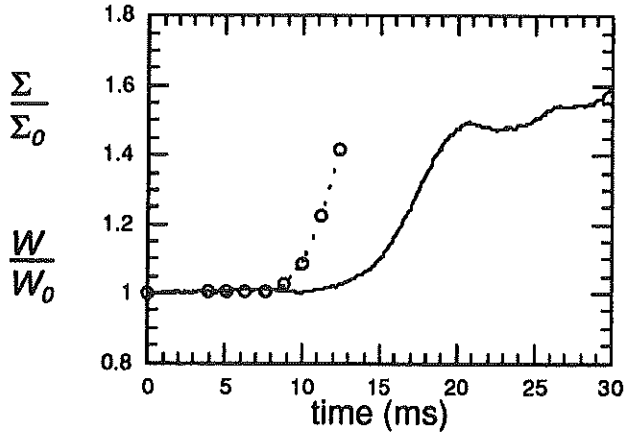

FIGURE 4. Evolution of W/W_0 (——) and Σ/Σ_0 (o), where W is the overall reaction rate, Σ is the total flame surface area, and the subscript 0 refers to the value at time $t = 0$. The operating conditions are the same as in Fig. 3.

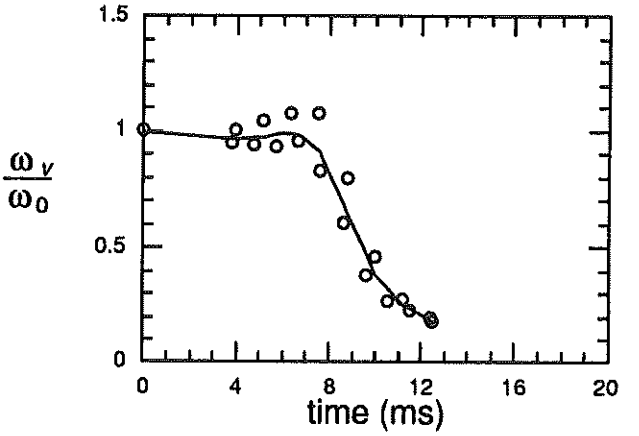

FIGURE 5. Evolution of ω_v/ω_0, where ω_v is the mean reaction rate per unit surface along the distorted flame front, and ω_0 is the initial value of ω_v. The operating conditions are the same as in Fig. 3.

quantified by defining ω_v as the average value of ω along the distorted part of the flame front. We obtain:

$$\frac{\omega_v}{\omega_0} = \frac{W_v}{\Sigma_v} \times \frac{\Sigma_0}{W_0}$$

with

$$W_v = W - W_0(1 - D/\Sigma_0) \quad \text{and} \quad \Sigma_v = \Sigma - \Sigma_0(1 - D/\Sigma_0)$$

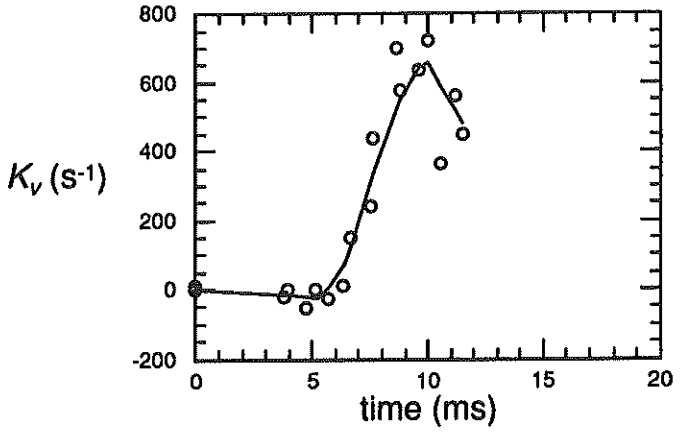

FIGURE 6. Evolution of mean stretch rate along the distorted flame front (K_v). The operating conditions are the same as in Fig. 3.

where ω_0, W_0, and Σ_0 are the initial values of the local reaction rate, of the global reaction rate, and of the flame surface area, respectively, and D is the size of the vortex pair $= 12\,mm$, as measured on the schlieren images. W_v and Σ_v represent the reaction rate and flame surface area of the portion of the flame affected by the vortex. It appears that ω_v decreases significantly to 20% of the initial value at the end of the first phase (Fig. 5). Similarly, an average value K_v for the stretch rate along the distorted front can be estimated by:

$$K_v = \frac{1}{\Sigma_v}\frac{d\Sigma_v}{dt}$$

Figure 6 shows that K_v reaches a maximum value of about 700 s^{-1} at $t = 10\,ms$. In comparison, the stretch rate leading to the extinction of a propane-air flame at $\phi = 0.55$, measured experimentally by Law *et al.* 1986 for a steady counterflow configuration, is an order of magnitude lower. Although unsteady effects, inherent of the present experiment, may play an important role and lead to different values of the extinction stretch rate, as indicated by Darabiha's work on the transient behavior of counterflow hydrogen-air diffusion flames (Darabiha 1992), the previous observation suggests that the flame front ahead of the vortex pair is quenched by excessive stretching. The same argument applies for various cases with the propane flame, where u_θ/S_l was varied between 90 and 350 (the corresponding maximum stretch rates varied from 400 s^{-1} to 1500 s^{-1}).

In order to study the effect of the Lewis number, experiments also have been performed on a methane-air flame. The operating conditions were: fuel= CH_4, $\phi = 0.55$, $V_0 = 0.35\,m/s$, $\delta_l = 2\,mm$, $S_l = 0.07\,m/s$, $d_c = 3\,mm$, $u_\theta = 11$ and $24\,m/s$, $Le = 0.96$.

In this case, the relationship between W and Σ changes when varying the ratio u_θ/S_l. When $u_\theta/S_l = 160$ ($u_\theta = 11\,m/s$), W is approximately proportional to Σ during most of the first phase, and when $u_\theta/S_l = 340$ ($u_\theta = 24\,m/s$), there is a

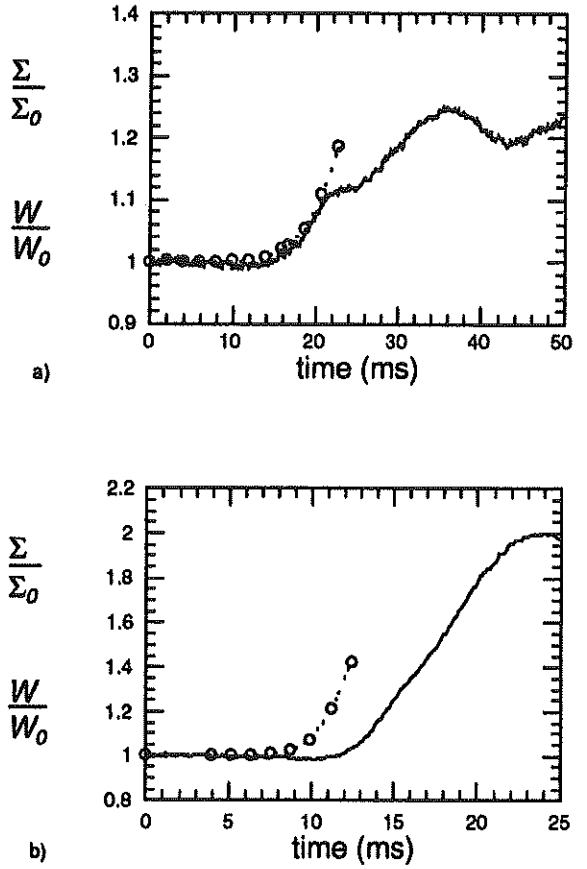

FIGURE 7. Methane-air flame. Evolution of W/W_0 (———) and Σ/Σ_0 (o), where W is the overall reaction rate, Σ is the total flame surface area, and the subscript 0 refers to the value at time $t = 0$. The conditions are: fuel = CH_4, $\phi = 0.55$, $V_0 = 0.35\,m/s$, $\delta_l = 2\,mm$, $S_l = 0.07\,m/s$, $d_c = 3\,mm$, $Le = 0.96$. a) $u_\theta = 11\,m/s$ $(u_\theta/S_l = 160)$. b) $u_\theta = 24\,m/s$ $(u_\theta/S_l = 340)$

time lag between W and Σ, as observed in the propane flame (Fig. 7 a and b). A transition in the response of the flame occurs when the vortex strength is increased. This difference in behavior can be seen in ω_v, the average value of the reaction rate: ω_v remains practically constant for the slower vortex pair, whereas it decreases significantly for the faster vortex pair (Fig. 8). The different behavior is due to a difference in stretch rates during the interaction. For $u_\theta/S_l = 340$, K_v reaches values of 800 s^{-1}, whereas for $u_\theta/S_l = 160$, K_v remains under 200 s^{-1}, and even under 100 s^{-1} during most of the first phase. Since the extinction stretch rate of a methane-air flame at $\phi = 0.55$ is around 100-200 s^{-1}, it can be concluded that, in the case of the faster vortex, the flame is locally quenched by excess of stretch. In contrast, in the case of the slower vortex, the stretch rate experienced by the flame front is lower or of the order of the extinction stretch rate. The local reaction rate

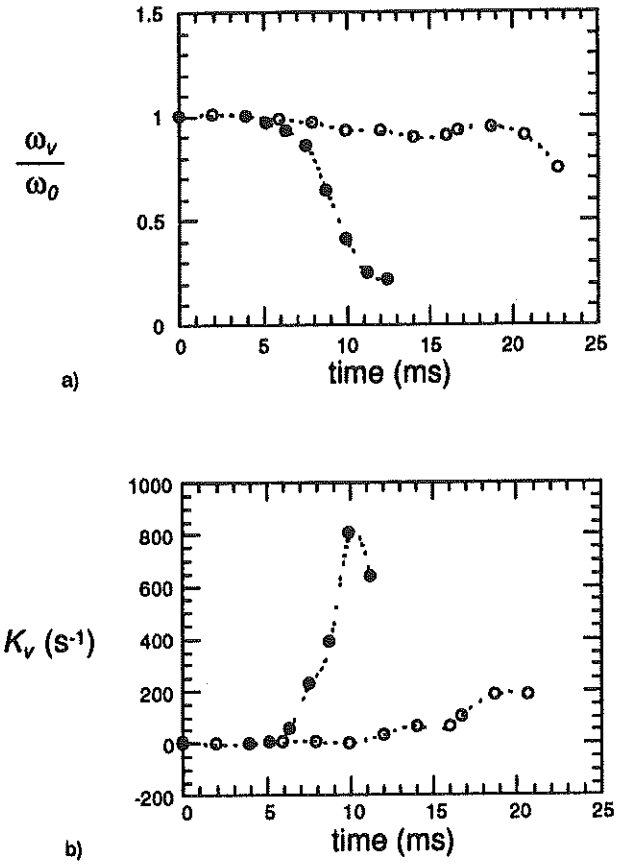

FIGURE 8. Methane-air flame for two values of u_θ/S_l. o : $u_\theta/S_l = 160$; • : $u_\theta/S_l = 340$. a) Evolution of ω_v/ω_0, where ω_v is the mean reaction rate per unit surface along the distorted flame front, and ω_0 is the initial value of ω_v - b) Evolution of mean stretch rate along the distorted flame front (K_v). The operating conditions are the same as in Fig. 7.

is weakly affected and W is approximately proportional to Σ.

The different response of the propane- and methane-air flames can be attributed to some extent to an effect of the Lewis number. During the interaction, both flames are positively stretched, and as suggested by the stretched flame theory, a positively stretched $Le > 1$ flame should be quenched more easily than a $Le < 1$ flame (Clavin 1985, Law 1988, Chung and Law 1988, Chung and Law 1989). Following Law, we obtain:

$$\omega_v/\omega_0 = 1 - \frac{\delta_l}{R_v} + (\frac{1}{Le} - 1)\frac{Ka}{(2T_{ad}/T_a)}$$

where ω_0 is the initial reaction rate, R_v is the average radius of curvature ($R_v > 0$ when the flame front is convex towards the burnt gases, and $R_v < 0$ when the

flame front is convex towards the cold gases), Ka is the Karlovitz number defined by $Ka = \frac{K_v}{S_l/\delta_l}$, T_{ad} is the adiabatic flame temperature, and T_a is the activation temperature. The influence of curvature is a consequence of flow divergence through a flame front having a finite thickness and does not involve the Lewis number. This term has probably the same influence on both the propane- and methane-air flames, hence its effect is not discussed here. In contrast, the influence of stretch on the flame response depends on the Lewis number. When $Le > 1$, the reaction rate is decreased by a positive stretch and quenching occurs by cooling of the flame. This is the case of the propane flame for which $Le = 1.8$. When $Le < 1$ or close to 1 which is the case of the methane flame, the mechanism for quenching is not so well established. When positively stretched, the flame will experience an increase of its burning rate and of its temperature. Stretch-induced quenching may or may not be expected depending on whether the flame is considered restrained or unrestrained (Law 1988). If the flame is restrained, for example in a stagnation point flow, the flame is quenched by incomplete reaction (Darabiha *et al.* 1986, Law 1988). If the flame is unrestrained, which is the case in the experiment, incomplete reaction is prevented: quenching cannot result only from excessive stretching, but more likely from the combination of stretch with other phenomena such as heat loss and finite-rate kinetics. To summarize, it appears that the effect of the Lewis number explains why the propane flame is quenched more easily than the methane flame, but it does not provide a definite explanation for the quenching of the methane flame.

It is interesting to note that Poinsot *et al.* 1991, in their numerical study of flame-vortex interactions, have found that radiative heat losses are the controlling mechanism for flame quenching irrespective of the value of the Lewis number. Following this analysis, Roberts *et al.* 1993 have characterized the effect of radiative heat losses from the burnt gases in their experiment, and although showing that Poinsot *et al.* had overestimated the value of the heat losses in their simulations, concluded that they play an important role in flame quenching. The authors also reported an unexpected finding: they would observe quenching in the case of a lean methane-air, but not in the case of a lean propane-air flame. This is in contradiction with our own findings as well as with the stretched flame theory. They attributed this apparent anomaly to complex chemistry effects. It appears that the mechanisms leading to flame quenching are not yet well established, and that this problem needs further investigations.

3. Future plans

Further investigations of the mechanisms controlling the flame response are being conducted. In particular, the effects of the Lewis number and of heat losses will be studied. Future experiments will involve quantitative imaging of the reaction rate field using an intensified CCD camera equipped with a filter isolating the radiation of CH radicals. A particle image velocimetry system will provide the velocity field, and imaging of the near-infrared radiation of water vapor will be used for the measure of the temperature field in the burnt gases. Comparison with direct numerical simulations will be performed in order to study separately the effects of non-unity

Lewis number, heat losses, and complex chemistry. The validity and applicability of reduced chemical schemes for direct numerical simulation of turbulent premixed flames will also be tested.

Acknowledgments

This work is conducted in collaboration with Prof. C. T. Bowman of the High Temperature Gasdynamics Laboratory. Helpful discussions with Prof. W. C. Reynolds and Prof. M. G. Mungal are also gratefully acknowledged. In addition, I wish to thank Dr. T. Poinsot (C.E.R.F.A.C.S., Toulouse, France), Dr. A. Trouvé and Dr. T. Mantel, (Center for Turbulence Research), for their encouragement and for valuable discussions during the course of this project. I also want to express my gratitude to F. Levy for his invaluable help during the construction of the experimental facility.

REFERENCES

BORGHI, R. 1988 Turbulent Combustion Modelling. *Prog. Energy Combust. Sci.* **14,** 245-292.

CHUNG, S. H. & LAW, C. K. 1988 An Integral Analysis of the Structure and Propagation of Stretched Premixed Flames. *Combust. Flame.* **72,** 325-336.

CHUNG, S. H. & LAW, C. K. 1989 Analysis of Some Nonlinear Premixed Flame Phenomena. *Combust. Flame.* **75,** 309-323.

CLAVIN, P. 1985 Dynamic behavior of premixed flame fronts in laminar and turbulent flows. *Prog. Energy Comb. Sci.* **11,** 1-59.

DARABIHA, N. 1992 Transient Behavior of Laminar Counterflow Hydrogen-Air Diffusion Flames With Complex Chemistry. *Combust. Sci. Tech.* **86,** 163-181.

DARABIHA, N., CANDEL, S. & MARBLE, F. E. 1986 The effect of strain rate on a premixed laminar flame. *Combust. Flame.* **64,** 203-217.

DIEDERICHSEN, J. & GOULD, R. D. 1965 Combustion Instability: Radiation from Premixed Flames of Variable Burning Velocity. *Combust. Flame.* **9,** 25-31.

HURLE, I. R., PRICE, R. B., SUGDEN, T. M., THOMAS, F. R. S. & THOMAS, A. 1968 Sound Emission From Open Turbulent Premixed Flames. *Proc. Roy. Soc. A.* **303,** 409-427.

JAROSINSKI, J., LEE, J. & KNYSTAUTAS, R. 1988 Interaction of a Vortex Ring and a Laminar Flame. *Twenty-Second Symposium (International) on Combustion,* The Combustion Institute, 505-514.

JOHN, R. & SUMMERFIELD, M. 1957 Effect of Turbulence on Radiation Intensity From Propane-Air Flames. *Jet Propul.* **27,** 169-178.

LAW, C. K. 1988 Dynamics of Stretched Flames. *Twenty-Second Symposium (International) on Combustion,* The Combustion Institute, 1381-1402.

LAW, C. K., ZHU, D. L. & YU, G. 1986 Propagation and Extinction of Stretched Premixed Flames. *Twenty-First Symposium (International) on Combustion,* The Combustion Institute, 1419-1426.

LEE, T.-W., LEE, J. G., NYE, D. A. & SANTAVICCA, D. A. 1993 Local Response and Surface Properties of Premixed Flames During Interactions with Kármán Vortex Streets. *Combust. Flame.* **94,** 146-160.

LEE, T.-W. & SANTAVICCA, D. A. 1993 Flame Front Geometry and Stretch During Interactions of Premixed Flames with Vortices. *Combust. Sci. Tech.* **90,** 211-230.

POINSOT, T., TROUVÉ, A., VEYNANTE, D., CANDEL, S. & ESPOSITO, E. 1987 Vortex Driven Acoustically Coupled Combustion Instabilities. *J. Fluid Mech.* **177,** 265-292.

POINSOT, T., VEYNANTE, D. & CANDEL, S. 1991 Quenching processes and premixed turbulent combustion diagrams. *J. Fluid Mech.* **228,** 561-605.

ROBERTS, W. L. & DRISCOLL, J. F. 1991 A Laminar Vortex Interacting with a Premixed Flame : Measured Formation of Pockets of Reactants. *Combust. Flame.* **87,** 245-256.

ROBERTS, W. L., DRISCOLL, J. F., DRAKE, M. C. & GOSS, L. P. 1993 Images of the Quenching of a Flame by a Vortex - To Quantify Regimes of Turbulent Combustion. *Combust. Flame.* **94,** 58-69.

RUTLAND, C. J. & FERZIGER, J. H. 1991 Simulations of Flame-Vortex Interactions. *Combust. Flame.* **84,** 343-360.

SAMANIEGO, J.-M. 1993 Generation of Two-Dimensional Vortices in a Cross-Flow. *CTR Annual Research Briefs - 1992.* Stanford Univ./NASA Ames.

SAMANIEGO, J.-M., YIP, B., POINSOT, T. & CANDEL, S. 1993 Low-Frequency Combustion Instability Mechanisms in a Side-Dump Combustor. *Combust. Flame.* **94,** 363-380.

WILLIAMS, F. A. 1985 *Combustion Theory.* The Benjamin/Cummings publishing Company, Inc.

WU, M.-S. & DRISCOLL, J. F. 1992 A Numerical Simulation of a Vortex Convected Through a Laminar Premixed Flame. *Combust. Flame.* **91,** 310-322.

YIP, B. & SAMANIEGO, J.-M. 1992 Direct C_2 Radical Imaging in Combustion Instabilities. *Combust. Sci. Tech.* **84,** 81-90.